Photochemical ageing drives the browning of urban outflows through secondary brown carbon production

Alejandra Velazquez-Garcia[1], Chenjie Yu[2], Sarah Tinorua[1*], Hichem Bouzidi [2], Eleonora Aruffo[3], Piero Di Carlo[4], Peter DeCarlo[5], Benjamin A. Nault[5,6,7], Thierry Bourrianne[1], Kevin Tu[2**], Edouard Pangui[2], Diana L. Pereira[2***], Mathieu Cazaunau[2], Ludovico Di Antonio[8****], Guillaume Siour[8], Matthias Beekmann[2], Astrid Bauville[2*****], Christopher Cantrell[8], Paola Formenti[2], Vincent Michoud[2] and Cyrielle Denjean[1].

[1]Météo-France, CNRS, Univ. Toulouse, CNRM, Toulouse, France
[2]Université Paris Cité et Univ Paris Est Creteil, CNRS, LISA, F-75013, Paris, France.
[3]University "G. d'Annunzio" of Chieti-Pescara, Department of Science, Center for Advanced Studies and Technology (CAST), Chieti, Italy
[4]University "G. d'Annunzio" of Chieti-Pescara, Department of Advanced Technologies in Medicine & Dentistry (DTM&O), Center for Advanced Studies and Technology (CAST), Chieti, Italy
[5]Department of Environmental Health and Engineering, Johns Hopkins University, Baltimore, United States
[6]Institute for Planetary Health, Johns Hopkins University, Baltimore, United States
[7]Center for Aerosol and Cloud Chemistry, Aerodyne Research, Inc., Billerica, United States
[8]Université Paris Est Creteil et Université Paris Cité, CNRS, LISA, F-94100, Creteil, France.
[*]now at Institute of Applied Geosciences, Technical University Darmstadt, Darmstadt, Germany
[**]now at Safran Aircraft Engines/Akkodis, 77550 Moissy-Cramayel, France.
[***]now at Institute for Atmospheric and Earth System Research / Physics, Faculty of Science, University of Helsinki, Helsinki, 00014, Finland
[****]now at LATMOS/IPSL, Sorbonne Université, UVSQ, CNRS, 75252 Paris, France
[*****]now at Muséum national d'Histoire naturelle (MNHN, CNRS), BioArch, Paris

Correspondence to : Alejandra Velazquez-Garcia (ale-vg13@hotmail.com) and Cyrielle Denjean (cyrielle.denjean@meteo.fr)

Table S1. Count of data points per instrument onboard of the aircraft and identified within plume conditions during ACROSS field campaign reported per flight number.

Flight number	Date	Number of data points for each instrument and flight						BC (µg m^{-3})	
		SP2 (1 sec)	A2S2 (10 sec)	Mini-AMS (15 & 20s)	PTR-ToF-MS (30 and 90 s)	TEI 49i TL analyser (5 s)	TD-LIF (1 sec)	75th percentile (in-plume)	25th percentile (background)
F26	21/June/2022	5958	805	526	126	6089	12361	0.159	0.107
F28	23/June/2022	8014	790*	411	123	5622	11866	0.127	0.071
F29	25/June/2022	3176	301	ND	43	3725	4320	0.116	0.047
F30	27/June/2022	6395	830	ND	126	3089	12503	0.138	0.053
F32	29/June/2022	5503	647	544	128	3045	12439	0.141	0.059
F33	01/July/2022	8172	652	517	125	2690	12325	0.092	0.030
F34	02/July/2022	5230	531	500	129	2819	12382	0.062	0.049
F35	04/July/2022	5629	585	703	127	3762	12413	0.056	0.040
F36	05/July/2022	4489	465	579	122	2881	ND	0.148	0.067

*Issues with measurements for A2S2 at 450 nm
ND: No data available

Table S2. Kruskal-Wallis tests and Dunn's post-hoc analysis performed on the $AAE_{450\text{-}630nm}$ values grouped by three O_x/BC ratio bins for in plume conditions.

O_x/BC ratio center bin	38.7	46.6	55.1
38.7	1	0.07	0.00
44.6	0.07	1	0.10
55.1	0.00	0.10	1

With a Kruskal-Wallis test we obtained a p-valor of 0.00000

Table S3. Variable loadings for the first four calculated principal components (PC1–PC4).

	PC1	PC2	PC3	PC4
O_x/BC	0.442	-0.444	0.778	-0.049
OA/BC	0.279	0.893	0.346	-0.065
C8 aromatics/toluene	-0.595	0.072	0.422	0.680
Photochemical age	0.611	-0.017	-0.310	0.728

Table S4. Median values of the observed parameters per O_x/BC bin used to calculate BrC production rate using a linear equation. The $AAE_{450\text{-}630nm}$ increases linearly with plume age over the 2–8 h (6 hours) period, corresponding to a slope of 0.25 h^{-1}. Using a linear parameterization (AAE = mt + b) and the first aging bin (t = 2 h, AAE = 1.1), the intercept is estimated as b = 0.60, yielding AAE(t) = 0.25t + 0.60. The sensitivity of AAE to the OA/BC ratio is given by d(AAE)/d(OA/BC) = 0.83, to the C8 aromatics/toluene ratio by d(AAE)/d(O_x/BC) = 0.091 and to the C8 aromatics/toluene ratio by d(AAE)/d(OA/BC) = -0.0053.

Median values per bin of Ox/BC ratio					
Bin tresholds	**Photochemical age (hours)**	**$AAE_{450\text{-}630nm}$**	**OA/BC ($\mu g\ m^{-3}$ / $\mu g\ m^{-3}$)**	**O_x/BC (ppbv / $\mu g\ m^{-3}$)**	**C8 aromatics/toluene (pptv / pptv)**
<44	2.0	1.1	3.7	38.7	351.5
>44 x >50	6.7	1.6	4.3	44.6	115.7
>=50	8.0	2.6	5.5	55.1	70.9
# of points (N) per bin of Ox/BC ratio					
<44	36	24	13	44	41
>44 x >50	10	9	11	13	10
>=50	6	25	30	30	13

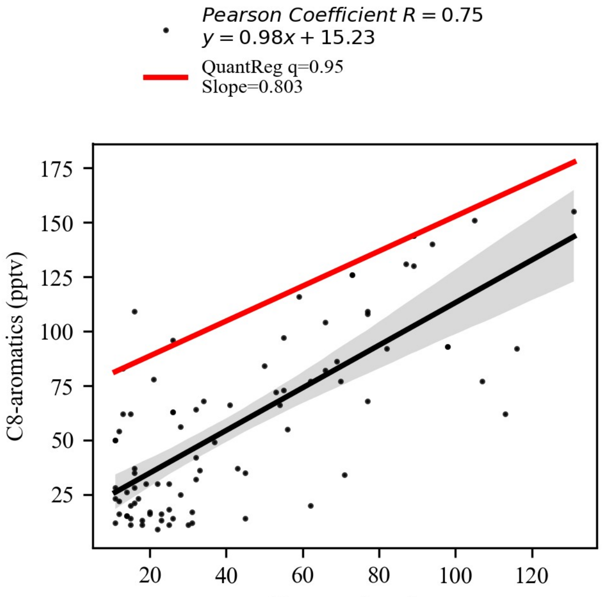

Figure S1. Scatterplot of C8 aromatics vs. benzene in the Paris plume. The red line is the slope of the steeper line fitting the upper limit of the scatterplot envelop. A value of 0.80 pptv/pptv has been set. The black line and the shaded areas are the linear fit. P-value: 0.0000.

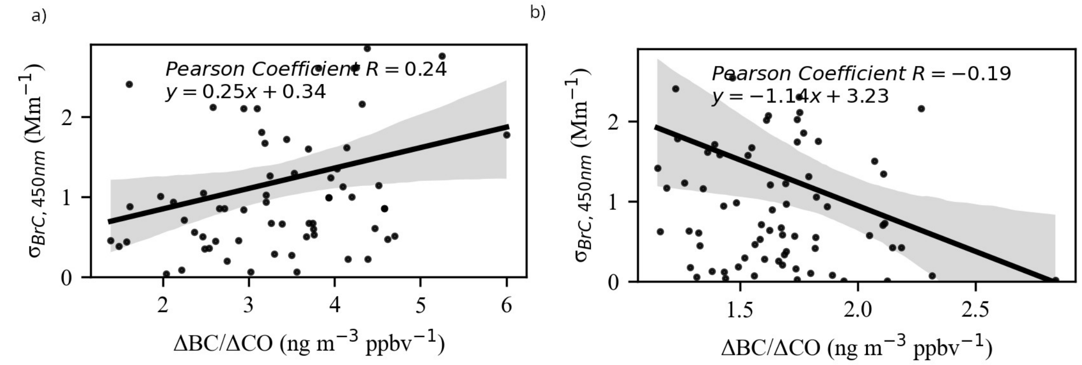

Figure S2. Correlations between brown carbon absorption coefficient and the emission ratio ΔBC/ΔCO for flight-portions identified within plume (a) and background (b) conditions.

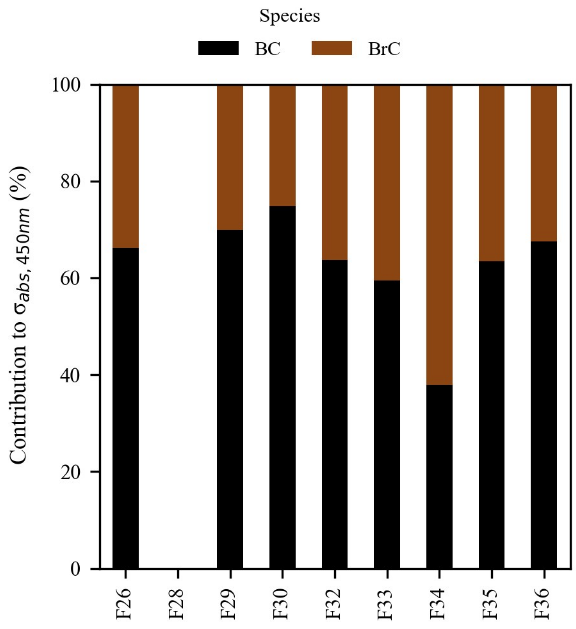

Figure S3. Light-absorbing carbonaceous aerosol contribution per flight number for in plume conditions.

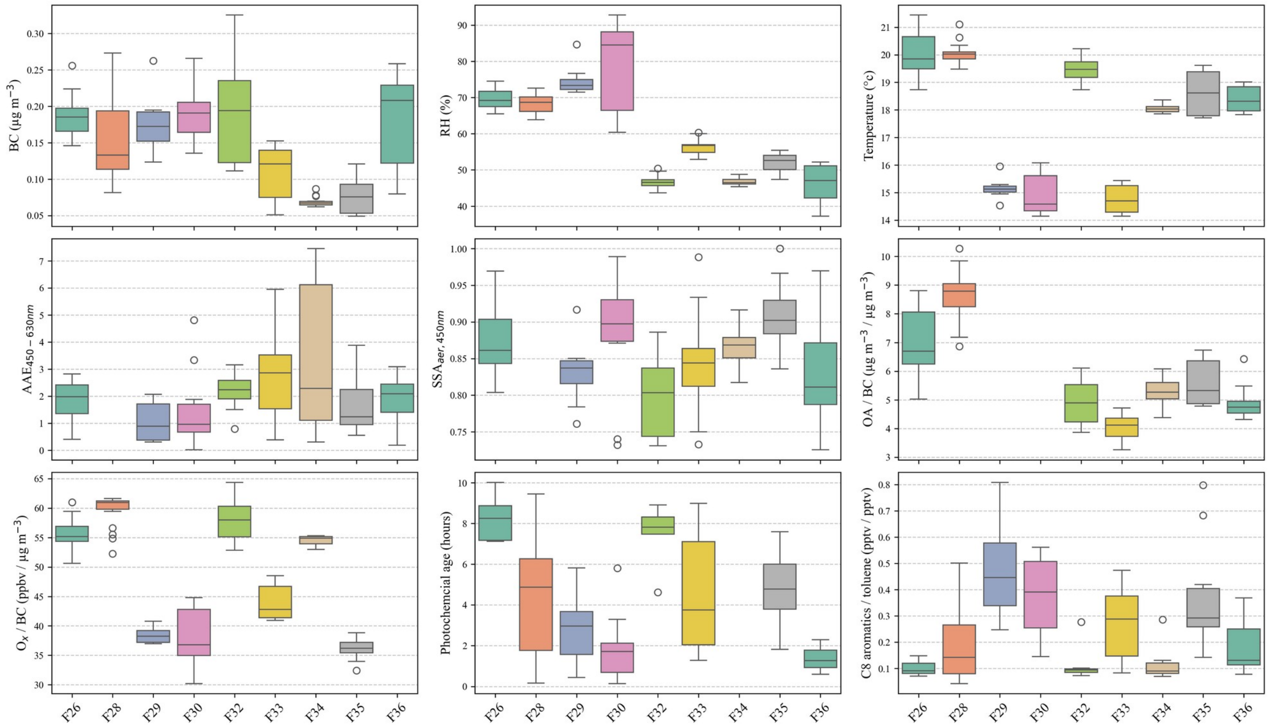

Figure S4. Box plots of the measured parameters (BC mass concentration, relative humidity, temperature, $AAE_{450-630nm}$, $SSA_{aer,450nm}$, OA-to-BC ratio, O_x-to-BC ratio, photo-chemical age, C8 aromatics-to-toluene ratio) onboard of the aircraft during ACROSS field campaign reported per flight number discussed in this work.

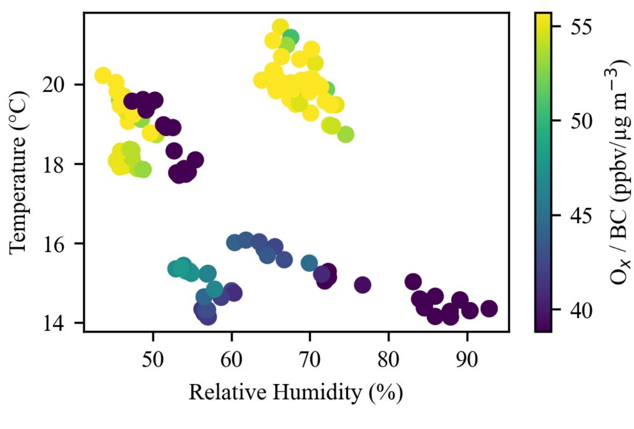

Figure S5. Relationship between the normalized oxidant ($O_x = O_3 + NO_2$) mixing ratio and the meteorological parameters for in plume conditions.

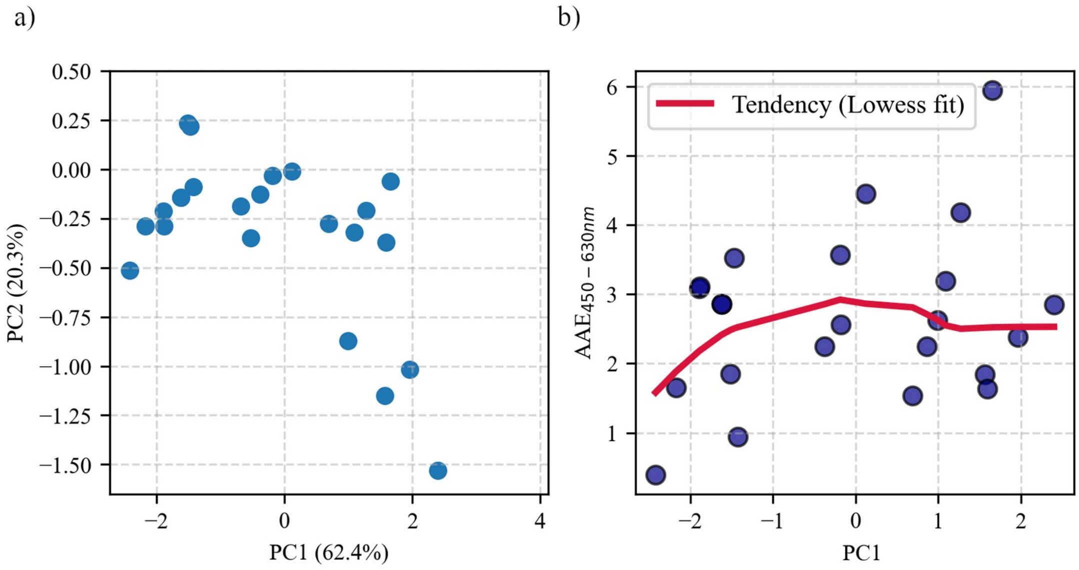

Figure S6. Principal Component Analysis of the urban plume aging and its relationship with aerosol optical properties. (a) Score plot showing the projection of data points onto the first two orthogonal principal components (PC1 and PC2), which account for 62.4% and 20.3% of the total atmospheric variance, respectively. (b) Absorption Angstrom Exponent plotted as a function of PC1, representing the photochemical clock. Individual observations (blue circles) are overlaid with a non-parametric Locally Weighted Scatterplot Smoothing regression line (red solid curve, smoothing fraction = 0.6) to highlight the iinitial secondary production followed by a tentative plateau/bleaching regime BrC.